PCCP

Physical Chemistry Chemical Physics

www.rsc.org/pccp

Volume 14 | Number 26 | 14 July 2012 | Pages 9237–9522

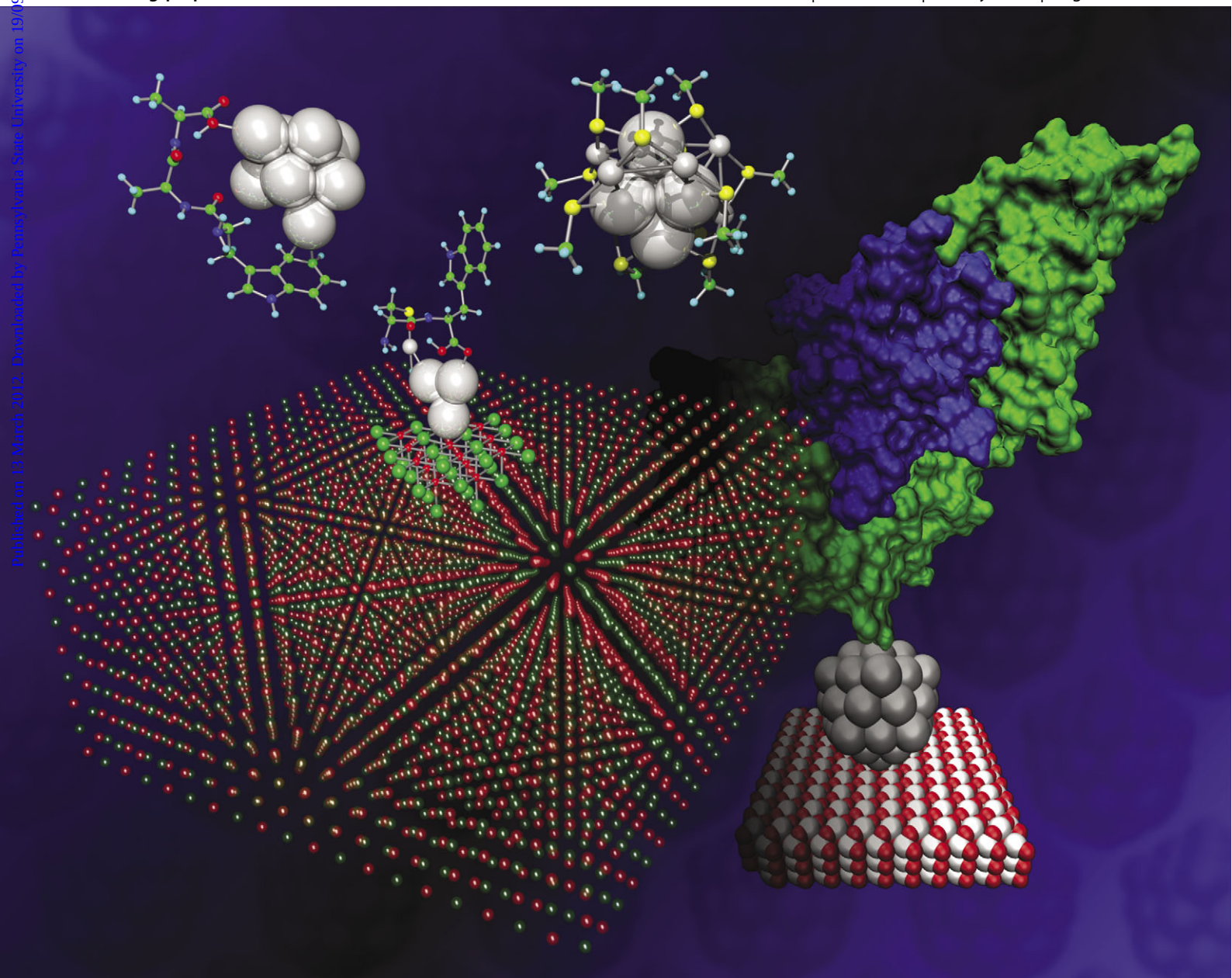

Includes a collection of articles on the theme of structure and reactivity of small particles

ISSN 1463-9076

COVER ARTICLE
Bonačić-Koutecký *et al.*
Silver cluster–biomolecule hybrids: from basics towards sensors

PCCP

View Article Online
Dynamic Article Links

Cite this: *Phys. Chem. Chem. Phys.*, 2012, **14**, 9282–9290

www.rsc.org/pccp

PERSPECTIVE

Silver cluster–biomolecule hybrids: from basics towards sensors

Vlasta Bonačić-Koutecký,*[ab] Alexander Kulesza,[c] Lars Gell,[a] Roland Mitrić,[c] Rodolphe Antoine,[de] Franck Bertorelle,[de] Ramzi Hamouda,[de] Driss Rayane,[de] Michel Broyer,[de] Thibault Tabarin[de] and Philippe Dugourd[de]

Received 7th January 2012, Accepted 17th February 2012
DOI: 10.1039/c2cp00050d

We focus on the functional role of small silver clusters in model hybrid systems involving peptides in the context of a new generation of nanostructured materials for biosensing. The optical properties of hybrids in the gas phase and at support will be addressed with the aim to bridge fundamental and application aspects. We show that extension and enhancement of absorption of peptides can be achieved by small silver clusters due to the interaction of intense intracluster excitations with the π–π* excitations of chromophoric aminoacids. Moreover, we demonstrate that the binding of a peptide to a supported silver cluster can be detected by the optical fingerprint. This illustrates that supported silver clusters can serve as building blocks for biosensing materials. Moreover, the clusters can be used simultaneously to immobilize biomolecules and to increase the sensitivity of detection, thus replacing the standard use of organic dyes and providing label-free detection. Complementary to that, we show that protected silver clusters containing a cluster core and a shell liganded by thiolates exhibit absorption properties with intense transitions in the visible regime which are also suitable for biosensing applications.

[a] *Department of Chemistry, Humboldt-Universität zu Berlin, Brook-Taylor-Str. 2, 12489 Berlin, Germany. E-mail: vbk@chemie.hu-berlin.de; Fax: +49 (0)30 2093-5573; Tel: +49 (0)30 2093-5579*
[b] *Interdisciplinary Center for Advanced Sciences and Technology (ICAST), University of Split, Meštrovićevo šetalište 45, HR-2100 Split, Republic of Croatia*
[c] *Department of Physics, Free University Berlin, Arnimallee 14, 14195 Berlin, Germany. E-mail: mitric@zedat.fu-berlin.de*
[d] *Université de Lyon, F-69622, Lyon, France*
[e] *Université Lyon 1, Villeurbanne, CNRS, UMR5579, LASIM, France. E-mail: dugourd@lasim.univ-lyon1.fr*

1 Introduction

Unique electronic and optical properties of metallic nanoparticles combined with the functionality of biomolecules led to the development of novel hybrid materials which became an important part of nanobiotechnology.[1–4] The metallic nanoparticles are responsible for significant enhancement of photoabsorption and emission of chromophores.[5,6] Since fluorescence labelling is a widely used technology in biosensing,[7–9] the role of

Vlasta Bonačić-Koutecký

Vlasta Bonačić-Koutecký is professor of physical and theoretical chemistry at the Humboldt Universität zu Berlin and director and founder of the Interdisciplinary center for advanced science and technology (ICAST) at the University of Split (Croatia). She studied physics at the University of Zagreb, received PhD in theoretical chemistry at the Johns Hopkins University (USA) and habilitation at the Freie Universität Berlin (Germany). Her research fields presently include theoretical photochemistry and its control by laser fields, metal clusters and their hybrids with biomolecules, simulation of time-resolved phenomena and development of cluster-based optical, biosensing and catalytic materials. She has published over 250 papers.

Roland Mitrić

Roland Mitrić has obtained PhD in theoretical chemistry from the Humboldt-Universität zu Berlin in 2003. Since 2009 he is an Emmy-Noether fellow at the Physics Department of the Freie Universität Berlin leading a junior research group. His research field includes the development and application of methods for the simulation and control of ultrafast dynamics in complex systems and cluster chemistry and physics. He is author of more than 90 publications.

metal particles gained significant importance due to their enhancement of fluorescence in hybrids. Usually, extrinsic organic fluorophores that can specifically label biomolecules have been used for detection.[10,11] Therefore, the idea of label-free detection by metallic nanoparticles that can replace such labeling compounds and increase the sensitivity of detection[12,13] became very attractive in the context of numerous applications.[14] The most widely used label-free detection technique is based on surface plasmon resonance (SPR) using thin metal films of gold[15] and silver.[16] However, optical detection and sensitivity is strongly dependent on the size and shape of nanoparticles[17,18] as well as on their intrinsic metallic properties. The strong localized enhancement of optical absorption and emission[19] as well as biocompatibility[20–22] are important factors that have to be fulfilled. In this context, small noble metal clusters in the nonscalable size regime with discrete electronic states exhibiting unique structure-dependent strong absorption and emission in the visible and UV range[23–26] are good candidates for replacing organic dyes such as chromophores. In fact, small silver clusters forming hybrids with peptides substantially extend and enhance optical absorption of pure peptides as shown in theoretical and experimental studies in the gas phase.[27–32] Moreover, due to the large s–d energy gap in silver, the localization of enhanced absorption in hybrid systems is significant due to s-electron excitations within the silver subunit. In contrast, in the case of gold clusters, the relativistic effects responsible for the small s–d gap permit excitations of d electrons. This leads to optical transitions of similar intensities spread over a large energy interval.[32] Therefore, in the context of localization of strong absorption in a narrow wavelength regime, silver clusters have preferable optical properties. Also a number of successful applications of silver clusters in cell imaging[20–22] and single molecule spectroscopy[33–35] have been reported. Concerning the investigation of metallic biomolecule hybrid systems in the condensed phase, the systems involving gold clusters have been considerably more extensively studied than those with silver clusters. The gold clusters have been successfully used to immobilize proteins at surfaces allowing to build ordered arrays[4] that were used in the production of biochips, in which only standard organic dyes have been employed for detection.[36] Also liganded gold clusters have been produced more than a decade ago and further intensively experimentally and theoretically investigated.[37–52] Their fluorescence properties with different ligands were also reported.[53] In contrast, the successful preparation of liganded silver clusters has been achieved only recently[54–57] and their fluorescence properties with different ligands were investigated.[58,59]

In this perspective feature contribution we focus on the role of silver clusters in hybrid systems following the concept from basics towards sensors. First, the gas-phase investigation of structural and optical properties of silver cluster–peptide hybrid systems will be addressed. It provides fundamental insight into the binding between metal clusters and peptides and into the mechanism of coupling of electronic excitations in hybrid systems. The joint theoretical and experimental work in the gas phase serves as an important prerequisite for proposing

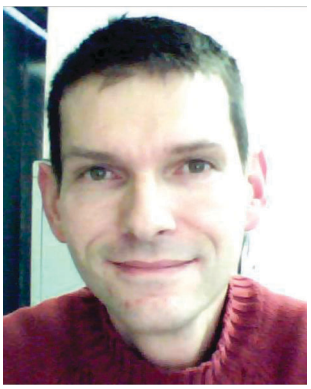

Rodolphe Antoine

Rodolphe Antoine is a senior scientist at the French National Center for Scientific Research (CNRS) and the University of Lyon I. He graduated in atomic and molecular physics and received the PhD in molecular physics at the University of Lyon I. His current interests focus on complex systems in the gas phase. He pioneered molecular beam deflection experiments to measure electric dipoles of biomolecules, laser-induced dissociation of trapped molecules and electron photodetachment dissociation for structural characterization of proteins. Presently, he is developing innovative couplings between mass spectrometry and laser spectroscopy for nanoobjects.

Michel Broyer

Michel Broyer studied Physics at Ecole Normale Supérieure de Paris and obtained a PhD at Laboratoire Kastler Brossel in Paris. In 1980, he became Professor in physics at University Lyon-1 where he developed research on molecular physics, metallic clusters, nanophysics and clusters/biomolecules complexes and spectroscopy of single nanoparticles. His awards include the Langevin prize of the French Academy of Sciences, the French German Gentner Kastler prize and the Humboldt Gay-Lussac Award. He has published about 300 papers. He is a senior member of the Institut Universitaire de France (IUF).

Philippe Dugourd

Philippe Dugourd is a senior scientist at the French National Center for Scientific Research (CNRS) and the University of Lyon. He graduated from the Ecole Normale Supérieure of Paris in Quantum Chemistry, and received PhD in molecular physics from the University of Lyon. His research is centred on determining the structure and dynamics of complex systems in the gas phase by using mass spectrometry, laser spectroscopy and ion mobility methods. His current interests focus on the conformation of proteins and on optical properties of metal–protein nanohybrids. He also develops new mass spectrometry methods and applications with the analytical chemistry department.

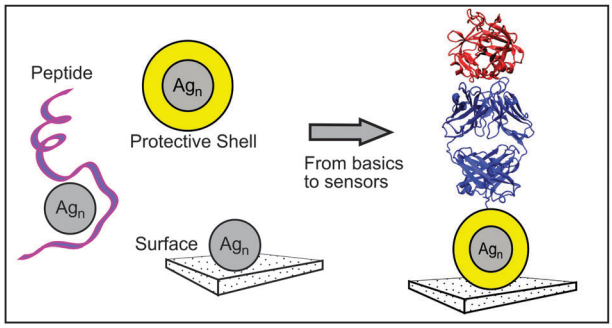

Fig. 1 Schematic representation of silver clusters interacting with different surroundings following the concept from basics (left) to sensors (right).

suitable building blocks for biomarkers. In order to proceed towards applications, the hybrid systems studied in the gas phase have to be stabilized or protected (*cf.* Fig. 1). This can be achieved by investigating the optical properties of hybrids at surfaces and of liganded clusters, respectively. In this context the silver–peptide hybrids at support can be considered as models towards the realization of label-free biosensing. For this purpose, the silver clusters should have double role, to immobilize biomolecules giving rise to ordered arrays and simultaneously to be used for detection due to their strong absorption and fluorescence. In addition, the silver clusters protected by thiolate ligands represent an alternative route for bioanalytical applications, since their easy surface functionalization and tuneable optical properties can be used for sensing in living cells. The small size of the clusters associated with an appropriate peptide sequence could greatly improve the penetration through the cell membrane.

Following the above outlined concept, we present first results on optical properties of silver cluster–peptide hybrid systems in the gas phase showing absorption enhancement of peptides by small silver clusters. Furthermore, we address optical properties of a silver cluster–dipeptide hybrid system at defect centers of MgO in order to illustrate that the comparison with the spectrum of the supported cluster allows us to identify the spectroscopic fingerprint of the peptide. Finally, the optical properties of a prototype for thiolate-liganded silver clusters that contain a silver cluster core with confined electrons will be presented. The choice of these model systems serves to outline and propose perspective features.

2 Computational and experimental

The structural and optical properties of the gas phase hybrid systems as well as of liganded clusters have been determined using density functional theory (DFT) and its time-dependent version (TDDFT).

For the silver atoms the 19-e$^-$ relativistic effective core potential (19-e$^-$ RECP) from the Stuttgart group[60] taking into account scalar relativistic effects has been employed. For all atoms triple zeta plus polarization atomic basis sets (TZVP) have been used.[60,61] Becke's three-parameter non-local exchange functional together with the Lee–Yang–Parr gradient-corrected correlation functional (B3LYP[62–65]) and its Coulomb-attenuated version (CAM-B3LYP[66]) have been employed to determine structural and optical properties of gas-phase hybrids and liganded clusters, respectively.

An extensive search for structures of the silver hybrid systems was performed using the simulated annealing method coupled to molecular dynamics simulations in the frame of the semiempirical AM1 method.[67] The found structures were then reoptimized in the frame of the DFT method using the functionals and AO basis sets as described above. The vibrational frequencies have been computed in order to find true minima on the potential energy surfaces.

The ionic MgO support was modelled by an embedded cluster approach in which a quantum mechanically (QM) described MgO cluster is embedded into a classical polarizable environment of point charges.[68] The QM part consists of a diamond-shaped $Mg_{13}O_{13}$ section of the MgO (100) surface. Mg^{2+} cations are introduced at the boundary of the QM model in order to avoid strong polarization by neighboring positive point charges, finally resulting in a $Mg_{13}O_{13}(Mg^{2+})_{16}$ QM subunit. Removing the central five-fold coordinated surface O atom leads to the creation of an F_S center defect (F_{5c}). The boundary Mg^{2+} cations have been described by effective core potentials from Hay and Wadt,[69] replacing the 1s, 2s and 2p electrons, while the valence 3s electrons are described by a single s-AO basis function contracted from two s-type primitive functions. For details describing the embedding of the QM subunit in an array of point charges as well as for determination of the structural properties of the supported clusters and supported hybrid systems compare ref. 70 in this issue and ref. 71. The optical properties for optimized structures of supported systems have been also calculated with the TDDFT method as those of free hybrid systems and liganded clusters.

Gas phase experiments were performed using a quadrupole ion trap mass spectrometer, coupled to an electrospray ion source and an UV-Vis optical parametric oscillator tunable laser.[72,73] The laser is injected at the center of the ion trap. The complexes were obtained from an electrolyte solution that was prepared by mixing a solution of silver salt and a peptide solution.[74] Electrospraying this solution leads to the formation of metal–peptide complexes. Specific complex (*i.e.* Trp-GlyAg_3^+) ions were then obtained by collisional activation of precursor complexes, isolated and irradiated in the quadrupole ion trap. The yield of fragmentation (Y) is given by $Y = \ln((parent + \sum frag)/parent)/F$, where F is the laser fluence, *parent* is the intensity of the precursor peak and $\sum frag$ represents the total intensity of the photofragment peaks.

Protected silver clusters were synthesized by reducing silver thiolates with $NaBH_4$ in the presence of excess glutathione (GSH) as reported by Bigioni and co-workers.[55] The raw product was separated using polyacrylamide gel electrophoresis (PAGE). Absorption spectra of different sizes of clusters were recorded using bands within the gel employing an Avantes spectrophotometer.

3 Results and discussion

The gas-phase approach on small prototypes is valuable since it allows the theoretical and experimental study of well defined systems without the influence of the environment. Exploration of optical properties of isolated silver cluster–peptide hybrid

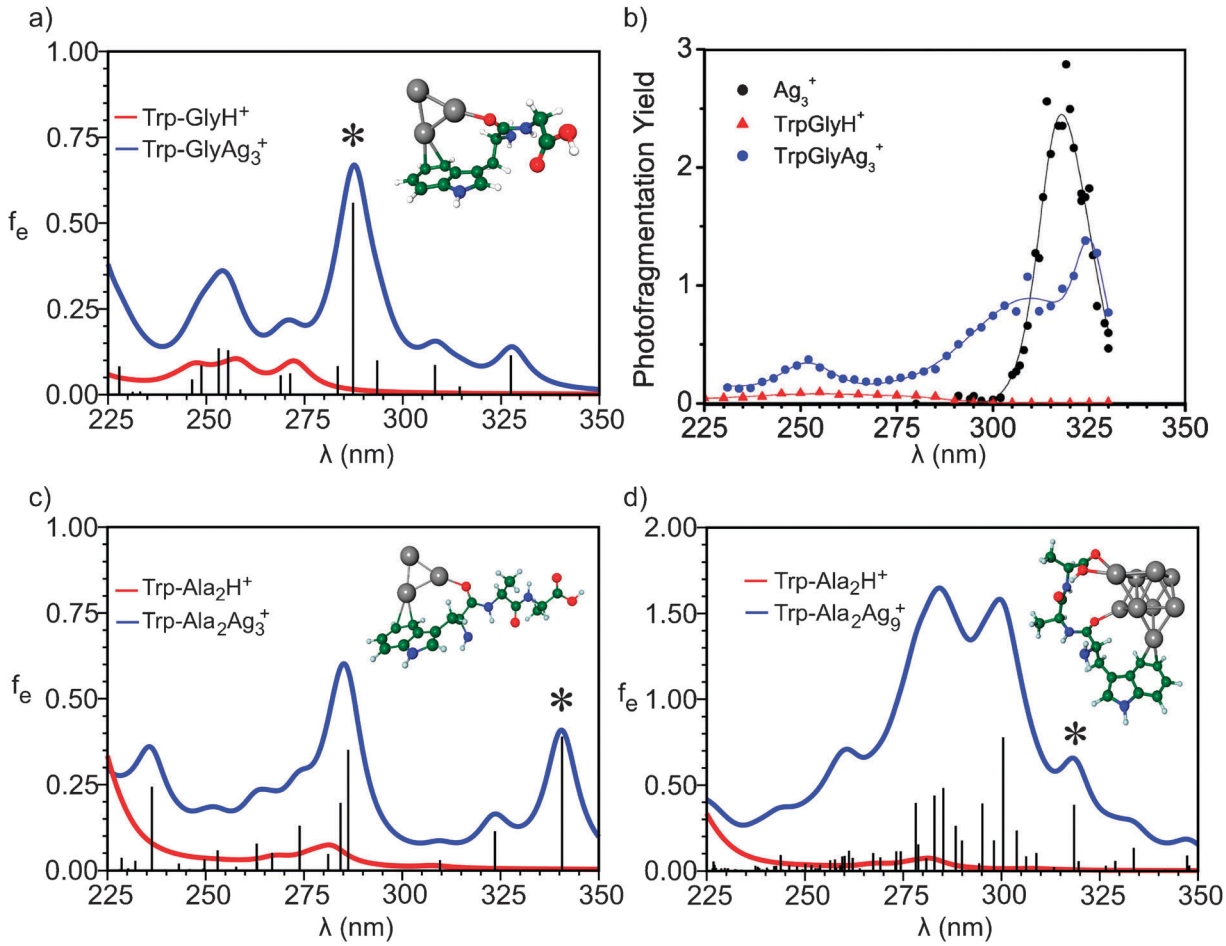

Fig. 2 Comparison of calculated absorption spectrum of the pure protonated dipeptide (Trp-GlyH$^+$) and tripeptide (Trp-Ala$_2$H$^+$) (red lines) with absorption spectra of hybrid systems with Ag_3^+ (a and c) and with Ag_9^+ (d) clusters (blue line). Broadening of the lines is simulated by the Lorentzian function with a half-width of 20 nm. The calculated oscillator strengths (f_e) for hybrid systems are drawn as black sticks. Analysis of transitions labeled by * is given in Fig. 3. (b) Experimental photofragmentation yields for protonated dipeptide (red triangles), bare Ag_3^+ (black dots) and Trp-GlyAg_3^+ hybrid (blue dots) as a function of wavelength. The solid lines serve to guide the eye.

systems at the molecular level was performed in order to rationalize the enhancement of absorption that is induced by metallic particles. For this purpose, we compare absorption spectra of pure peptides with those obtained for cluster–peptide hybrids as shown in Fig. 2. We consider cationic hybrids since the charged systems are experimentally accessible.[28–31] The chosen prototype examples contain Trp-Gly dipeptide and Trp-Ala$_2$ tripeptide with two cluster sizes Ag_3^+ and Ag_9^+. The purpose is to identify the structures and to show that enhancement of absorption is present for systems with both cluster sizes, independent of the peptide length. Moreover, Fig. 2b displays also experimental fragmentation yields of the Trp-GlyAg_3^+ hybrid system and two isolated subunits. This allows comparison with theoretical results of Fig. 2a and provides the proof of principle. Since the spectroscopic pattern is strongly dependent on the structural properties, the calculated lowest-energy structures are also shown for all three systems in Fig. 2. The presence of the metal cluster reduces significantly the conformational flexibility of the peptides. Structures are of "charge-solvated" nature in which positively charged silver clusters are bound to free electron pairs of oxygen atoms and to the π-system of the indole ring, thus allowing the interaction of excitations within the cluster and within the indole ring. The absorption spectrum calculated for the lowest-energy isomer of Trp-GlyAg_3^+ shown in Fig. 2a exhibits two pronounced bands centered around 250 and 290 nm. The intense band at 290 nm is due to a series of electronic transitions resulting from the coupling of S → $P_{x,y}$ cluster-type of excitations within the Ag_3^+ subunit with charge transfer excitations between Ag_3^+ and indole subunits. The electron density difference between the electronic ground and excited state at 288 nm presented in Fig. 3a shows that the major charge redistribution after excitation takes place within Ag_3^+. The considerably less intense band centered at 250 nm is due to the coupling of the S → P_z excitation of Ag_3^+ (which is located around 215 nm in pure Ag_3^+) with the charge transfer excitation involving the indole subunit and the peptide bond. In summary, the strong optical absorption of the hybrid system, which originates mainly from the contribution of the Ag_3^+ cluster, thus, significantly extends and enhances the absorption of the peptide from the range of 250 nm into the near UV regime. Complementary to the theoretical investigation Fig. 2b displays experimental fragmentation yields of the protonated dipeptide (Trp-GlyH$^+$), the free Ag_3^+ cluster and

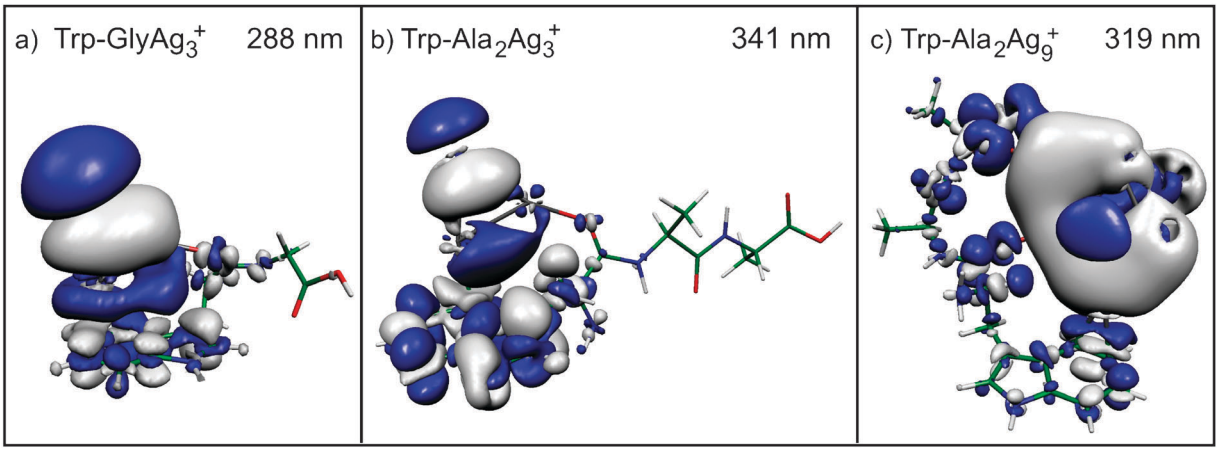

Fig. 3 Electron density difference between the electronically excited state and ground state (a) for $TrpGlyAg_3^+$ at 288 nm (b) for $Trp\text{-}Ala_2Ag_3^+$ at 341 nm and (c) for $Trp\text{-}Ala_2Ag_9^+$ at 319 nm corresponding to the transitions labeled by * in Fig. 2.

the spectrum of the hybrid system $Trp\text{-}GlyAg_3^+$. The protonated Trp-Gly dipeptide exhibits one absorption band centered around 255 nm which is characteristic for Trp-containing peptides and is due to excitation of the π-electrons within the indole ring. No fragmentation is observed above 295 nm. For the silver trimer cation one intense transition around 320 nm is observed, which is due to the degenerate $S \rightarrow P_{x,y}$ transition of Ag_3^+.[29] The experimental photofragmentation spectrum for $Trp\text{-}GlyAg_3^+$ exhibits two fragmentation bands between 225 and 330 nm. The less intense band around 255 nm is also present in the experimental spectrum of the protonated dipeptide, although with weaker intensity. The second band arises around 275 nm and continuously extends up to 325 nm. The intensity at the maximum of this band is lower than the recorded one for isolated Ag_3^+, but the photofragmentation is spread over a larger range of wavelengths. The agreement between theoretical and experimental results shown in Fig. 2a and b is of qualitative nature, due to the fact that experiments were carried out at $T = 300$ K and the presented theoretical results correspond to $T = 0$ K. If temperature-broadening is taken into account, the agreement is more quantitative as shown previously.[29] The above presented theoretical and experimental results show that the smallest silver clusters such as Ag_3^+ can serve as optical absorbing labels.

In order to illustrate that the concept is more general, we present the stable structures and corresponding calculated absorption spectra for $Trp\text{-}Ala_2Ag_3^+$ and for $Trp\text{-}Ala_2Ag_9^+$ in Fig. 2c and d, investigating the influence of the peptide length and cluster size on optical properties of hybrids. The absorption spectra of both hybrid systems, compared with the ones calculated for free protonated tripeptide, exhibit strong absorption enhancement and extension in the UV regime due to the presence of the clusters. Moreover, the intense transitions in the hybrid system with the Ag_9^+ cluster are one order of magnitude stronger than in the case of hybrids with Ag_3^+. The analysis of excitations responsible for intense transitions at 341 nm and 319 nm for Ag_3^+-tripeptide and Ag_9^+-tripeptide, given in Fig. 3b and c, respectively, shows that major charge redistribution after excitation takes place within the clusters. This is also the case for higher energy intense transitions below 275 nm. Therefore the conclusion can be drawn that gas-phase investigations of silver cluster–peptide hybrids strongly suggest that the role of clusters as local probes replacing commonly used organic dyes might be substantially advantageous, avoiding the chemical coupling of the peptides with the dyes and simultaneously increasing the sensitivity of the detection.

In order to proceed from basics towards sensors, we present structural and optical properties of one prototype example of a hybrid system at the support. We have chosen the neutral silver tetramer interacting with the dipeptide Cys-Trp supported at the F_S defect center of MgO. Our previous study of small noble metal clusters at the F_S defect center of the MgO support showed that the silver tetramer is a good candidate for an emissive center, because of long-living low-lying electronic excited states.[71] The cysteine-containing dipeptide has been chosen because proteins interact typically with metal particles *via* the sulfur atoms of the cysteine residue. Moreover, the defect center of MgO binds metal clusters and strongly stabilizes cluster–biomolecule hybrids. In the lowest energy structure of $Cys\text{-}TrpAg_4$ at the F_S center of MgO, one Ag atom is inserted into the sulfur–hydrogen bond of cysteine, the other one is bound to the carboxyl–oxygen atom of Trp and a third one is interacting with the F_S center of MgO, as shown in Fig. 4. The identification of an $Ag_4H\text{–}SCH_3$ subunit in the hybrid system implies that due to the electron withdrawing effect of the sulfur and oxygen atoms, two confined electrons in the Ag_3^+ subunit are present, Thus together with two electrons of the F_S center of MgO, systems with four confined electrons are formed. It is well known from our previous work that the dominant absorption transition for Ag_3^+ is located close to 300 nm and for the free Ag_4 cluster at 400 nm.[75] In Fig. 4a and b we compare the calculated absorption spectrum for the F_S center of MgO with the one obtained for $Cys\text{-}TrpAg_4$ at support. The dominant transition for the F_S center is located close to 350 nm. Consequently, the interaction between the hybrid system containing an Ag_3^+ subunit and the F_S center forming a system with four confined electrons should give rise to an absorption spectrum with a dominant transition close to 400 nm (in analogy to the spectrum of Ag_4). This is the case as shown in Fig. 4b. The analysis of the dominant transition at 397 nm confirms that excitations between the electrons from the F_S center and the Ag_3^+ subunit of the hybrid system occur,

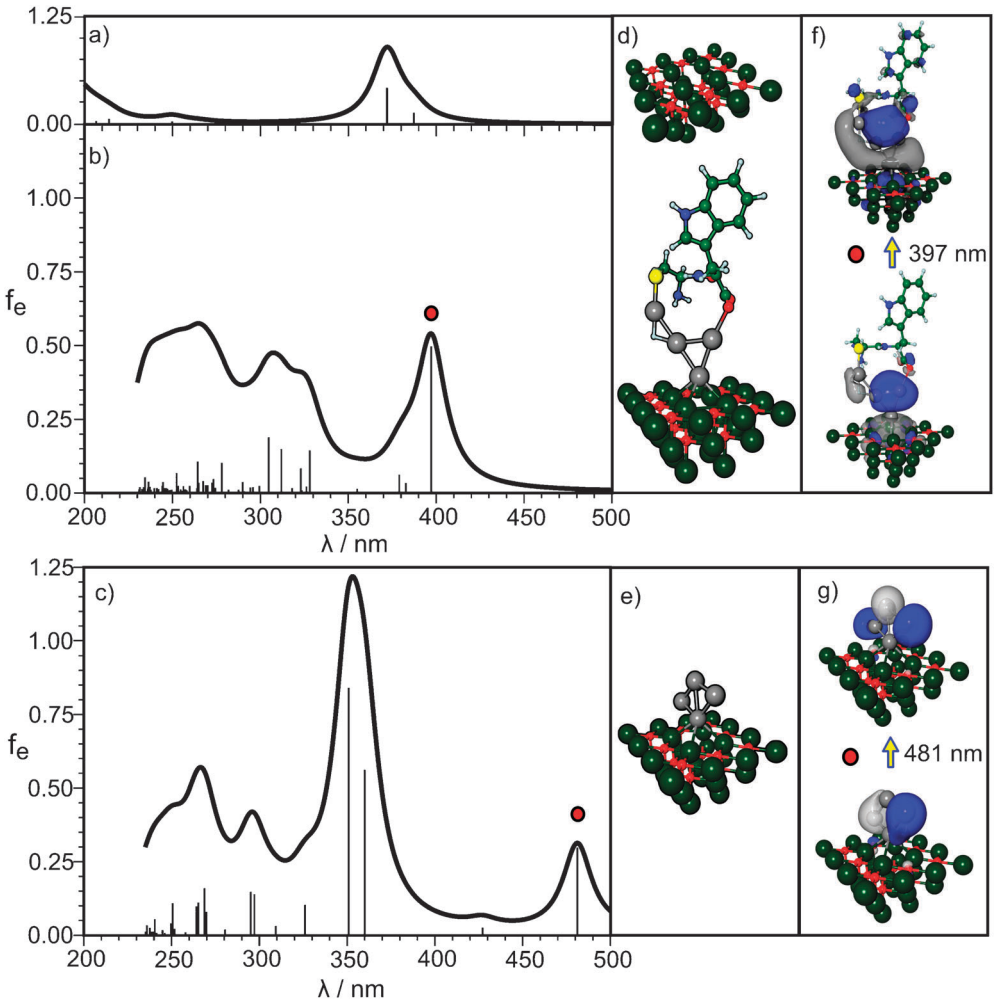

Fig. 4 Comparison between calculated spectra of (a) F_S defect center of MgO, (b) supported hybrid Cys-TrpAg$_4$ and (c) supported Ag$_4$ cluster. Broadening of the lines is simulated by the Lorentzian function with a half-width of 20 nm. The calculated oscillator strengths (f_e) are drawn as black sticks. (d) Structure of the F_S defect center of MgO and supported hybrid Cys-TrpAg$_4$ (only QM part is presented). (e) Structure of the supported Ag$_4$ cluster (only QM part is presented). Analysis of the marked transition in spectra of (f) supported hybrid and (g) supported cluster in terms of leading excitation between Kohn–Sham orbitals.

which confirms the qualitative considerations described above. In order to address the question how the supported silver cluster can be used to detect the binding of the dipeptide, we present in addition to the calculated spectrum of supported hybrid systems also the spectrum of the bare silver tetramer at support in Fig. 4c. The latter system is characterized by a low-lying transition at 480 nm and dominant transitions at 350 nm. This can be qualitatively considered as the fingerprint of systems with six confined electrons (four from the cluster and two from the F_S center of MgO). In fact, the leading features of the supported silver tetramer spectrum resemble the absorption of Ag_6.[23] The comparison of spectra of the supported hybrid with the one for the supported cluster (*cf.* Fig. 4b and c) shows explicitly that the appearance of the intense transition for the supported hybrid system at 400 nm is the signature of the presence of the Cys-Trp dipeptide. This means that the binding of peptides can be detected by the optical fingerprint, and thus supported silver clusters can serve as building blocks for biosensing materials.

Finally we wish to address the protection of clusters by ligands as another possibility for sensing applications. An example of silver clusters liganded by glutathione obtained following the Bigioni synthesis[55] is shown in Fig. 5a. The resolved bands in the inset of Fig. 5a correspond to different magic size clusters. The absorption spectrum of band 6 is also displayed in Fig. 5a. It exhibits a strong absorption peak at $\sim$500 nm. The absorption for Ag : SG clusters around 500 nm can have a great advantage for biological applications. The phototoxicity induced by an UV blue laser can be significantly reduced by an excitation in the visible range. To rationalize the effect of thiolated liganded shells on structural and optical properties of silver clusters, we present theoretical results obtained for a prototype example in Fig. 5b and c containing S–CH_3 ligands (see ref. 76 in this issue). Since sulfur can be considered as an electron acceptor, each pair of Ag and S atoms formally consists of Ag^+ and S^-. Thus, by combining n silver atoms and x ligands the excess of Ag atoms determines the count of confined electrons, which is similar to the "superatom" model used successfully for thiolate protected gold clusters.[52] In the case of anionic species, which are experimentally accessible, one additional electron has to be

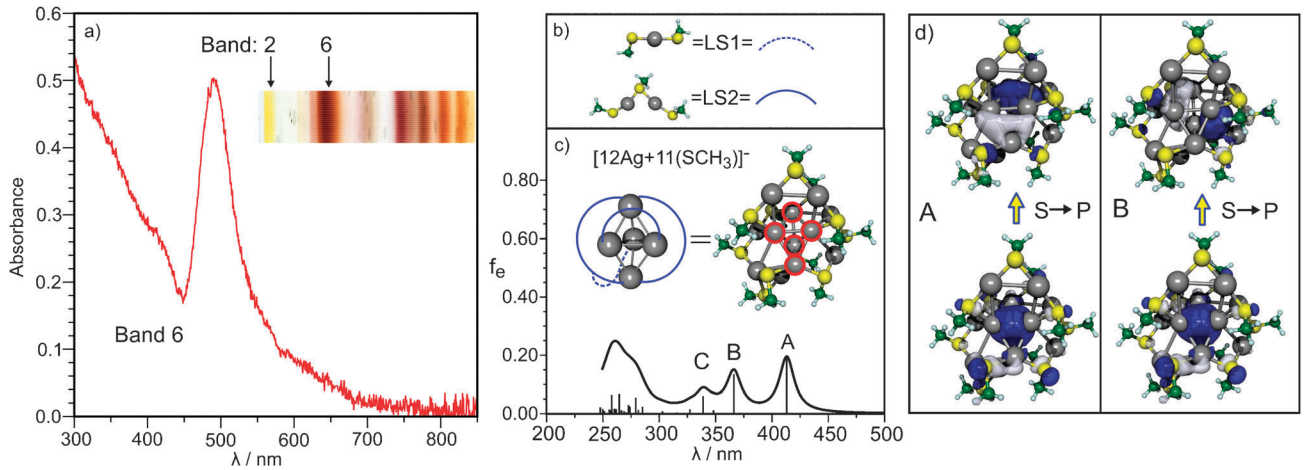

Fig. 5 (a) Optical absorption spectrum of the selected Ag:SG band (band 6 as labeled in ref. 55). This band contains mainly magic-size cluster with 31 silver atoms and 19 glutathione protected ligands. Inset: Bands from PAGE gel separation. (b) and (c) Structure and absorption spectrum of the $[12Ag + 11(SCH_3)]^-$ complex with an Ag_5 core protected by two types of ligands: LS1 and LS2. (d) Analysis of transitions labeled by A and B in terms of leading excitations between Kohn–Sham orbitals. S and P denote the nature of cluster-like orbitals of the Ag_5 core.

taken into account. Therefore anionic systems with n Ag atoms and $x = n - 1$ ligands contain two confined electrons. In the case of $n = 12$ and $x = 11$ the structure of the $[12Ag + 11(SCH_3)]^-$ complex contains an Ag_5 core which is protected by four ligands belonging to two different types. One ligand is of the type labeled by LS1 (CH_3S–Ag–SCH_3) and the other three ligands are of the type labeled by LS2 (CH_3S–Ag–SCH_3–Ag–SCH_3) as shown in Fig. 5b and c. Thus, the fully ligand-protected Ag_5 core containing two confined electrons plays an important role for determining the spectroscopic pattern as shown in Fig. 5c. The pattern is characterized by three intense transitions between 350 and 420 nm arising by excitations from the S-cluster-core orbital to the three components of P-cluster-core-orbitals labelled by A, B and C in Fig 5c. The analysis given in Fig 5d shows two components corresponding to A and B transitions. The first transition with considerable intensity is located close to 420 nm. Different ligands are likely to influence locations of the intense transitions which is important for sensing applications. Of course, the size and the structure of the core can also influence the details of the spectroscopic patterns. The question can be raised concerning the formation of liganded clusters for a given number of silver atoms and ligands. In this respect, we have chosen to present the $[12Ag + 11(SCH_3)]^-$ complex, which might be formed from $[nAg + (n + 1)(SCH_3)]^-$ systems by dissociation of two ligands according to preliminary energetic considerations.

Interestingly enough, for the chosen prototypes presented here, the absorption spectra of the supported silver–dipeptide hybrid as well as of the liganded silver cluster with an Ag_5 core exhibit intense transitions close to 400 nm which indicates convenient emissive properties in both cases. Thus, comparison with the optical properties of hybrid systems in the gas phase indicates strongly that the surrounding plays an important role, not only for stabilization or protection of the clusters, but also concerning the location of intense transitions. Therefore, the interplay between enhancement of absorption of biomolecules due to the metallic subunit and the surrounding is decisive for the design of systems with emissive properties suitable for sensing.

4 Conclusions and outlook

We have shown that the small silver clusters in the nonscalable size regime (<2 nm) can serve as optical probes for biomolecules. In contrast to quantum dots, low nuclearity silver clusters are highly attractive for applications due to their low toxicity and very small size, as recently reported on surfaces[77,78] and *in vivo*.[79] However, the synthesis, isolation and functionalization of size selected low nuclearity silver clusters are still a bottleneck. Since protected silver clusters are not as stable as analogous gold clusters, their identification by mass spectrometry, X-ray or nuclear magnetic resonance is still scarce. For example, it would be desirable to achieve X-ray determination of structures for ligand protected silver clusters in analogy to those obtained for gold.[80] In addition, the theoretical exploration of their structural and electronic properties as well as the mechanism for growth and stabilization are needed. Bioconjugation can provide extra functionality such as stability, biocompatibility and targeting. Moreover, fluorescent metallic nanoclusters could also be directly synthesized at the biological template[81–83] without further bioconjugation steps, thus opening a bright perspective for applications.

The basics gained from the gas phase studies serve to build up realistic model systems towards applications. There are two routes to proceed in the future. First, metallic clusters at support can be used to immobilize proteins in order to form ordered arrays and simultaneously provide enhanced fluorescent properties due to the coupling with the proteins. Thus, the ultimate goal is to realize label-free biosensing at the molecular level. This route leads towards the design of materials for biochips in which, for example, human serum can be poured over the biochip array and diagnostics with increased sensitivity can be achieved. The second route

concerns ligand-protected clusters which might be used for sensing and diagnostic in living cells. Both routes might profit from unique optical properties of small silver clusters.

Author contributions

Vlasta Bonačić-Koutecký has initiated and supervised the theoretical investigation of cluster–biomolecule hybrids, supported hybrid systems as well as liganded silver clusters and wrote the paper. Alexander Kulesza has performed calculations on cluster biomolecule–hybrids and supported hybrid systems. Lars Gell has performed calculations on liganded clusters. Roland Mitrić has contributed to interpretation of the theoretical results. Rodolphe Antoine and Philippe Dugourd have initiated and supervised the experiments on cluster–biomolecule hybrids and liganded clusters. Franck Bertorelle has contributed to the preparation of the liganded clusters. Ramzi Hamouda, Driss Rayane and Thibault Tabarin have contributed to experiments on cluster–biomolecule hybrid systems as well as on liganded clusters. Michel Broyer has initiated experiments on cluster–biomolecule hybrids.

Acknowledgements

We acknowledge long term stimulating and fruitful cooperation with L. Wöste and his team. Financial support by the Deutsche Forschungsgemeinschaft priority program SPP 1153 "Clusters at Surfaces: Electron Structure and Magnetism" and by the Project "Laboratoire International Associé (LIA)" between France and Croatia is gratefully acknowledged. A.K. and R.M. acknowledge the financial support in the framework of the "Emmy-Noether-Programme" (ENP-MI-1236) of the Deutsche Forschungsgemeinschaft (DFG).

References

1 E. Katz and I. Willner, *Angew. Chem., Int. Ed.*, 2004, **43**, 6042–6108.
2 M. E. Stewart, C. R. Anderton, L. B. Thompson, J. Maria, S. K. Gray, J. A. Rogers and R. G. Nuzzo, *Chem. Rev.*, 2008, **108**, 494–521.
3 R. Wilson, *Chem. Soc. Rev.*, 2008, **37**, 2028–2045.
4 R. E. Palmer and C. Leung, *Trends Biotechnol.*, 2007, **25**, 48–55.
5 J. R. Lakowicz, *Anal. Biochem.*, 2005, **337**, 171–194.
6 L. Zhao, L. Jensen and G. Schatz, *J. Am. Chem. Soc.*, 2006, **128**, 2911–2919.
7 C.-A. J. Lin, C.-H. Lee, J.-T. Hsieh, H.-H. Wang, J. K. Li, J.-L. Shen, W.-H. Chan, H.-I. Yeh and W. H. Chang, *J. Med. Biol. Eng.*, 2009, **29**, 276–283.
8 J. Yu, S. Choi, C. I. Richards, Y. Antoku and R. M. Dickson, *Photochem. Photobiol.*, 2008, **84**, 1435–1439.
9 L. Shang, S. Dong and G. U. Nienhaus, *Nano Today*, 2011, **6**, 401–418.
10 A. N. Kapanidis and S. Weiss, *J. Chem. Phys.*, 2002, **117**, 10953–10964.
11 R. Ando, H. Mizuno and A. Miyawaki, *Science*, 2004, **306**, 1370–1373.
12 J. R. Lakowicz, *Plasmonics*, 2006, **1**, 5–33.
13 E. G. Matveeva, T. Shtoyko, I. Gryczynski, I. Akopova and Z. Gryczynski, *Chem. Phys. Lett.*, 2008, **454**, 85–90.
14 N. Nath and A. Chilkoti, *J. Fluoresc.*, 2004, **14**, 377–389.
15 I. Gryczynski, J. Malicka, Z. Gryczynski and J. R. Lakowicz, *J. Phys. Chem. B*, 2004, **108**, 12568–12574.
16 J. R. Lakowicz, J. Malicka, I. Gryczynski and Z. Gryczynski, *Biochem. Biophys. Res. Commun.*, 2003, **307**, 435–439.
17 M. A. El-Sayed, *Acc. Chem. Res.*, 2001, **34**, 257–264.
18 K.-S. Lee and M. A. El-Sayed, *J. Phys. Chem. B*, 2006, **110**, 19220–19225.
19 E. Cottancin, G. Celep, J. Lerme, M. Pellarin, J. R. Huntzinger, J. L. Vialle and M. Broyer, *Theor. Chem. Acc.*, 2006, **116**, 514–523.
20 J. Yu, S. A. Patel and R. M. Dickson, *Angew. Chem., Int. Ed.*, 2007, **46**, 2028–2030.
21 J. Yu, S. Choi and R. M. Dickson, *Angew. Chem., Int. Ed.*, 2009, **48**, 318–320.
22 Y. Antoku, J.-i. Hotta, H. Mizuno, R. M. Dickson, J. Hofkens and T. Vosch, *Photochem. Photobiol. Sci.*, 2010, **9**, 716–721.
23 V. Bonačić-Koutecký, V. Veyret and R. Mitrić, *J. Chem. Phys.*, 2001, **115**, 10450–10460.
24 C. Sieber, J. Buttet, W. Harbich, C. Félix, R. Mitrić and V. Bonačić-Koutecký, *Phys. Rev. A*, 2004, **70**, 041201.
25 P. Radcliffe, A. Przystawik, T. Diederich, T. Döppner, J. Tiggesbäumker and K.-H. Meiwes-Broer, *Phys. Rev. Lett.*, 2004, **92**, 173403.
26 J. Zheng, P. R. Nicovich and R. M. Dickson, *Annu. Rev. Phys. Chem.*, 2007, **58**, 409–431.
27 I. Compagnon, T. Tabarin, R. Antoine, M. Broyer, P. Dugourd, R. Mitrić, J. Petersen and V. Bonačić-Koutecký, *J. Chem. Phys.*, 2006, **125**, 164326.
28 R. Mitrić, J. Petersen, A. Kulesza, V. Bonačić-Koutecký, T. Tabarin, I. Compagnon, R. Antoine, M. Broyer and P. Dugourd, *J. Chem. Phys.*, 2007, **127**, 134301.
29 T. Tabarin, A. Kulesza, R. Antoine, R. Mitrić, M. Broyer, P. Dugourd and V. Vlasta Bonačić-Koutecký, *Phys. Rev. Lett.*, 2008, **101**, 213001.
30 A. Kulesza, R. Mitrić and V. Bonačić-Koutecký, *J. Phys. Chem. A*, 2009, **113**, 3783–3788.
31 A. Kulesza, R. Mitrić, V. Bonačić-Koutecký, B. Bellina, I. Compagnon, M. Broyer, R. Antoine and P. Dugourd, *Angew. Chem., Int. Ed.*, 2011, **50**, 878–881.
32 A. Kulesza, R. Mitrić and V. Bonačić-Koutecký, *Chem. Phys. Lett.*, 2011, **501**, 211–214.
33 K. Kneipp, H. Kneipp, I. Itzkan, R. R. Dasari and M. S. Feld, *Chem. Phys.*, 1999, **247**, 155–162.
34 T. Sannomiya and J. Vörös, *Trends Biotechnol.*, 2011, **29**, 343–351.
35 G. Rong, H. Wang and B. M. Reinhard, *Nano Lett.*, 2010, **10**, 230–238.
36 A. A. Fisher, J. C. Nelson and D. Ure, *Genet. Eng. Biotechnol. News*, 2008, **28**, 28–29.
37 T. G. Schaaff, M. N. Shafigullin, J. T. Khoury, I. Vezmar, R. L. Whetten, W. G. Cullen, P. N. First, C. Gutiérrez-Wing, J. Ascensio and M. J. Jose-Yacamán, *J. Phys. Chem. B*, 1997, **101**, 7885–7891.
38 T. G. Schaaff, G. Knight, M. N. Shafigullin, R. F. Borkman and R. L. Whetten, *J. Phys. Chem. B*, 1998, **102**, 10643–10646.
39 R. L. Donkers, D. Lee and R. W. Murray, *Langmuir*, 2004, **20**, 1945–1952.
40 I. Hussain, S. Graham, Z. Wang, B. Tan, D. C. Sherrington, S. P. Rannard, A. I. Cooper and M. Brust, *J. Am. Chem. Soc.*, 2005, **127**, 16398–16399.
41 Y. Negishi, K. Nobusada and T. Tsukuda, *J. Am. Chem. Soc.*, 2005, **127**, 5261–5270.
42 A. P. Gies, D. M. Hercules, A. E. Gerdon and D. E. Cliffel, *J. Am. Chem. Soc.*, 2007, **129**, 1095–1104.
43 J. Kim, K. Lema, M. Ukaigwe and D. Lee, *Langmuir*, 2007, **23**, 7853–7858.
44 M. Zhu, E. Lanni, N. Garg, M. E. Bier and R. Jin, *J. Am. Chem. Soc.*, 2008, **130**, 1138–1139.
45 N. K. Chaki, Y. Negishi, H. Tsunoyama, Y. Shichibu and T. Tsukuda, *J. Am. Chem. Soc.*, 2008, **130**, 8608–8610.
46 R. Jin, *Nanoscale*, 2010, **2**, 343–362.
47 J. Akola, M. Walter, R. L. Whetten, H. Häkkinen and H. Grönbeck, *J. Am. Chem. Soc.*, 2008, **130**, 3756–3757.
48 H. Häkkinen, M. Walter and H. Grönbeck, *J. Phys. Chem. B*, 2006, **110**, 9927–9931.
49 C. M. Aikens, *J. Phys. Chem. Lett.*, 2011, **2**, 99–104.
50 M. Zhu, C. M. Aikens, F. J. Hollander, G. C. Schatz and R. Jin, *J. Am. Chem. Soc.*, 2008, **130**, 5883–5885.
51 Y. Pei, Y. Gao, N. Shao and X. C. Zeng, *J. Am. Chem. Soc.*, 2009, **131**, 13619–13621.
52 M. Walter, J. Akola, O. Lopez-Acevedo, P. D. Jadzinsky, G. Calero, C. J. Ackerson, R. L. Whetten, H. Grönbeck and

H. Häkkinen, *Proc. Natl. Acad. Sci. U. S. A.*, 2008, **105**, 9157–9162.
53 Z. Wu and R. Jin, *Nano Lett.*, 2010, **10**, 2568–2573.
54 N. Nishida, H. Yao, T. Ueda, A. Sasaki and K. Kimura, *Chem. Mater.*, 2007, **19**, 2831–2841.
55 S. Kumar, M. D. Bolan and T. P. Bigioni, *J. Am. Chem. Soc.*, 2010, **132**, 13141–13143.
56 Y. Cui, Y. Wang, R. Liu, Z. Sun, Y. Wei, Y. Zhao and X. Gao, *ACS Nano*, 2011, **5**, 8684–8689.
57 T. U. B. Rao, B. Nataraju and T. Pradeep, *J. Am. Chem. Soc.*, 2010, **132**, 16304–16307.
58 I. Diez and R. H. A. Ras, *Nanoscale*, 2011, **3**, 1963–1970.
59 T. Udaya Bhaskara Rao and T. Pradeep, *Angew. Chem., Int. Ed.*, 2010, **49**, 3925.
60 D. Andrae, U. Haeussermann, M. Dolg, H. Stoll and H. Preuss, *Theor. Chim. Acta*, 1990, **77**, 123.
61 S. Gilb, P. Weis, F. Furche, R. Ahlrichs and M. M. Kappes, *J. Chem. Phys.*, 2002, **116**, 4094–4101.
62 A. D. Becke, *J. Chem. Phys.*, 1993, **98**, 5648.
63 C. Lee, W. Yang and R. G. Parr, *Phys. Rev. B: Condens. Matter*, 1988, **37**, 785.
64 S. J. Vosko, L. Wilk and M. Nusair, *Can. J. Phys.*, 1980, **58**, 1200.
65 P. J. Stephens, F. J. Devlin, C. F. Chabalowski and M. J. Frisch, *J. Phys. Chem.*, 1994, **98**, 11623.
66 T. Yanai, D. P. Tew and N. C. Handy, *Chem. Phys. Lett.*, 2004, **393**, 51–57.
67 M. J. S. Dewar, E. G. Zoebisch, E. F. Healy and J. J. P. Stewart, *J. Am. Chem. Soc.*, 1985, **107**, 3902.
68 P. V. Sushko, A. L. Shluger and C. R. Catlow, *Surf. Sci.*, 2000, **450**, 153.
69 P. J. Hay and W. R. Wadt, *J. Chem. Phys.*, 1985, **82**, 284.
70 A. Kulesza, R. Mitrić and V. Bonačić-Koutecký, *Phys. Chem. Chem. Phys.*, 2012, DOI: 10.1039/C2CP23500E, Advance Article.
71 C. Bürgel, R. Mitrić and V. Bonačić-Koutecký, *Phys. Status Solidi B*, 2010, **247**, 1099–1108.
72 F. O. Talbot, T. Tabarin, R. Antoine, M. Broyer and P. Dugourd, *J. Chem. Phys.*, 2005, **122**, 074310.
73 V. Larraillet, R. Antoine, P. Dugourd and J. Lemoine, *Anal. Chem.*, 2009, **81**, 8410–8416.
74 T. Tabarin, R. Antoine, M. Broyer and P. Dugourd, *Eur. Phys. J. D*, 2006, **37**, 237–239.
75 V. Bonačić-Koutecký, J. Pittner, M. Boiron and P. Fantucci, *J. Chem. Phys.*, 1999, **110**, 3876.
76 L.-S. Wang, C.-G. Ning, X.-G. Xiong, Y.-L. Wang and J. Li, *Phys. Chem. Chem. Phys.*, 2012, DOI: 10.1039/C2CP23490D, Accepted Manuscript.
77 G. E. Johnson, C. Wang, T. Priest and J. Laskin, *Anal. Chem.*, 2011, **83**, 8069–8072.
78 G. E. Johnson, T. Priest and J. Laskin, *ACS Nano*, 2011, **6**(1), 573–582.
79 S. Choi, J. Yu, S. A. Patel, Y.-L. Tzeng and R. M. Dickson, *Photochem. Photobiol. Sci.*, 2011, **10**, 109–115.
80 P. D. Jadzinsky, G. Calero, C. J. Ackerson, D. A. Bushnell and R. D. Kornberg, *Science*, 2007, **318**, 430–433.
81 C. I. Richards, S. Choi, J.-C. Hsiang, Y. Antoku, T. Vosch, A. Bongiorno, Y.-L. Tzeng and R. M. Dickson, *J. Am. Chem. Soc.*, 2008, **130**, 5038–5039.
82 B. Han and E. Wang, *Anal. Bioanal. Chem.*, 2012, **402**, 129–138.
83 J. Xie, Y. Zheng and J. Y. Ying, *J. Am. Chem. Soc.*, 2009, **131**, 888–889.

